33RD CONGRESS
OF THE INTERNATIONAL COUNCIL
OF THE AERONAUTICAL SCIENCES
STOCKHOLM, SWEDEN, 4-9 SEPTEMBER, 2022

ICAS 2022 SWEDEN

ASSESSMENT AND CONTROL OF ARRIVAL FLOW AND WAITING TIME APPLYING GT/GI/ST+GI TIME-VARYING QUEUING MODEL

Koki Higasa[1] & Eri Itoh[1,2]

[1]The University of Tokyo, 7-3-1, Hongo, Bunkyo Ward, Tokyo 113-8656, Japan
[2]Electronic Navigation Research Institute, 7-42-23 Jindaiji higashi-machi, Chofu City, Tokyo 182-0012, Japan

Abstract

To propose operational strategies to control arrival traffic efficiently, the $G_t/GI/s_t + GI$ time-varying queueing model, which considers time-dependent factors, is employed to model the actual arrival aircraft traffic flow at Tokyo International Airport. A methodology for analyzing the arrival traffic flow in the enroute airspace is also proposed and applicable to various airports. Analytical results assuming various distributions of inter-arrival times indicated that earlier control in the upstream airspace can help reduce the hourly average delay time by up to 85% in the enroute airspace. The model and results can spawn future work that will verify that such control also mitigates congestion in the terminal airspace.

Keywords: time-varying queueing model, air traffic management, arrival management

1. Introduction

1.1 Background

An increase in air traffic is forecasted. [1] reports that the number of passenger and cargo jets in service will grow significantly by 2.3 and 2.0% per year, respectively, which will mean severe congestion for major airports with massive takeoffs and landings, impeding the smooth flow. This underlines the crucial need to control incoming aircraft efficiently in the terminal airspace and the surrounding enroute airspace, within runway capacity restrictions. Arrival Manager (AMAN), the system for supporting metering and vectoring, has been utilized. However, given distance-dependent uncertainty about calculating trajectories [2], uniform arrival management throughout the airspace cannot relieve congestion effectively.

Multi-Stage AMAN (see Fig. 1) can replace traditional AMAN. It intends to integrate independently operated subsystems divided by flight phases. Itoh et al. [2] indicated that advancing transitions between stages would be the optimum strategy in Tokyo International Airport, using actual flight data. Over 60% of the domestic flights use the airport [2].

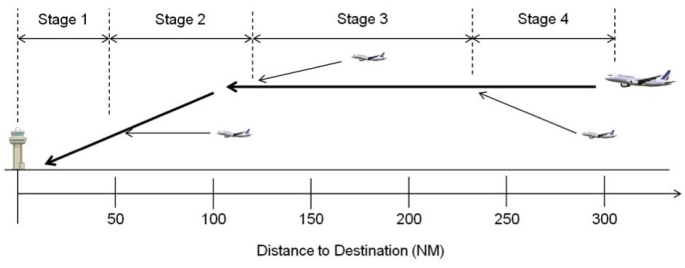

Figure 1 – Conceptual diagram of a possible Multi-Stage AMAN design [2].

In this context, Extended-AMAN (E-AMAN) has been developed, which manages arrival traffic over wide-ranging areas, including current enroute airspace. E-AMAN can ease the controller's workload, noise and fuel consumption more efficiently. Itoh et al. [3] described E-AMAN with four-dimensional trajectory-based operations to propose that E-AMAN should start at a distance of 100-150 NM from the airport. Note that analysis based on actual aircraft flow is necessary for proposing design principles since the E-AMAN design requirements vary with different airports, airspaces and air traffic characteristics.

This section is summarized as follows; data-driven analysis is required to determine where and how E-AMAN / Multi-Stage AMAN starts controlling the arrival flow and it should cover not only the airspace adjacent to the airport but also its surrounding airspace for the integrated system. However, few studies deal with the broad range of airspace, despite the fact that data-driven approaches have become mainstream.

1.2 Literature on Modeling Arrivals

Among techniques capable of covering wide-ranging operational research themes in air traffic, the queueing model, particularly with the Poisson arrival process, can directly investigate phenomena with stochasticity and non-stationarity in traffic [4]. Itoh and Mitici [5] focused on arrivals at Tokyo International Airport using the $M/G/c/K$ queueing model to propose strategies to reduce the delay time. A non-homogeneous Poisson model has also been employed to simulate airports or their networks [6] [7] [8] because arrival intervals can be considered as 'sufficiently random' [4]. However, [9] pointed out that the Poisson arrival process cannot be deemed appropriate for arrivals at the congested airport since the arrival flow is successively rearranged to follow air traffic controllers.

With this in mind, some researchers have been applying the Pre-Scheduled Random Arrivals (PSRA) model, which assumes the actual arrival time equates to the sum of pre-scheduled time and deviations therefrom. Besides [9], Gwiggner and Nagaoka [10] analyzed the air traffic flow arriving at Tokyo International Airport in the enroute area. They used the PSRA model and compared it with the Poisson model to find that they are similar in moderately congested circumstances and not those that are highly congested. The PSRA model can directly assess the impact of the lower deviation of arrival time, which would be impossible in the Poisson model, described only by a rate parameter [10].

1.3 Research Objective and Structure

Itoh and Mitici [5] examined both terminal and enroute airspace comprehensively, but the time-constant queueing model was unable to simulate actual arrival traffic flow with time-varying characteristics. Accordingly, this study applies a time-varying queueing model to develop general and comprehensive strategies for controlling the arrival flow from enroute airspace (the blue region in Fig. 4 below) to terminal airspace around Tokyo International Airport as a case study. Concretely, we introduce the $G_t/GI/s_t + GI$ queueing model, which can consider the time-dependent arrival rate and capacity with exceptional early departure, to assess delay time in the current enroute airspace and demonstrate the impact of arrival intervals with less deviation by setting virtual arrival flow in the area. This paper only covers the matters above, although the study will verify that the control in upstream airspace (the green region in Fig. 4 below) helps reduce delay of terminal airspace and ensure a more orderly landing flow. Using the $G_t/GI/s_t + GI$ queueing model, we can simulate wide-ranging arrival flows following various distributions and provide insights from a perspective other than that of the PSRA model. As far as we know, no literature adopts the model for the arrival flow (although Itoh et al. [11] do so for the surface flow).

The rest of the paper is organized as follows. In Section 2, the deterministic $G_t/GI/s_t+GI$ fluid model, which approximates the stochastic model, is introduced (Section 2.1) and two types of states and waiting times are incorporated (Section 2.2). Finally, the relationship between variables is illustrated and procedures for similar airspace are put forward (Section 2.3). In Section 3, the airspace, flow and flight data of interest are defined (Section 3.1) and policies on tuning parameters (e.g. arrival rate, service time distribution and capacity) are also described (Section 3.2). Finally, the methodology is summarized to connect the actual airspace and model with the original equation (Section 3.3). In Section 4, we analyze the current airspace to find that only certain periods are subject to delay. In Section 5, we focus our discussion on the arrival rate to clarify that arriving aircraft cannot be excessively controlled by air traffic controllers in advance. Eight scenarios of inter-arrival times from different distributions are considered. Finally, Section 6 sets out the conclusion and future work.

2. The $G_t/GI/s_t+GI$ Queueing Model

2.1 Outline of the Model

The conceptual diagram of the $G_t/GI/s_t+GI$ queueing model is presented in Fig. 2. It comprises the arrival process characterized by a time-varying arrival rate $\lambda(t)$ (G_t), an independent and identical distribution of service time $g(x)$ (GI), a time-varying capacity $s(t)$ (s_t) and an independent and identical distribution of abandon time $f(x)$ ($+GI$). This paper applies the deterministic fluid model, which approximates the stochastic queueing model, and expounds on each component based on Liu and Whitt [12]. We postulate that the service discipline is first-come-first-served. The arrival process is deterministically characterized by $\lambda(t)$. $Q(t)$, the quantity of fluid in a queue at time t, is

$$Q(t) = \int_0^\infty q(t,x)dx$$

where $q(t,x)$ is the density of fluid in a queue at time t for time less than or equal to x. $B(t)$, the quantity in a service at time t, is

$$B(t) = \int_0^\infty b(t,x)dx$$

where $b(t,x)$ is the density of fluid in a service at time t for time less than or equal to x, characterized by $g(x)$. Moreover, $\sigma(t)$, the quantity of fluid per unit time which exits the system at time t, is

$$\sigma(t) = \int_0^\infty b(t,x)\frac{g(x)}{\bar{G}(x)}dx$$

where

$$\bar{G}(x) = 1 - \int_0^x g(u)du$$

Finally, the cumulative distribution function of abandon time $F(x)$, the time before fluid leaves the system without receiving service, is

$$F(x) = \int_0^x f(u)du$$

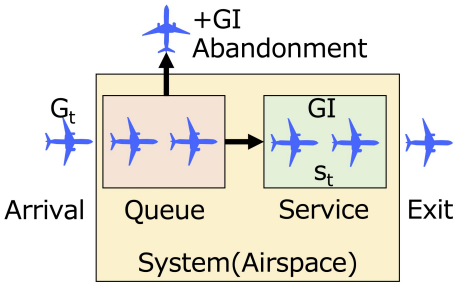

Figure 2 – Conceptual diagram of the $G_t/GI/s_t+GI$ queueing model.

2.2 States and Waiting Times

Depending on $\lambda(t)$ and $s(t)$, the system alternates between two intervals: overload ($Q(t) > 0$) and underload ($Q(t) = 0$). When the initial time is 0, each state transits to another one at times T_1 (overload) and T_2 (underload) if the system satisfies

$$T_1 = \inf\{u : Q(u) = 0, \lambda(u) \leq s'(u) + \sigma(u)\}$$
$$T_2 = \inf\{u : B(u) = s(u), \lambda(u) > s'(u) + \sigma(u)\}$$

Furthermore, we can define two waiting times:

- Boundary waiting time $w(t)$: Actual delay time of the head airplane in a queue at time t
- Potential waiting time $v(t)$: Virtual delay time of the airplane entering the airspace at time t

2.3 Summary of the Model and Iteration Steps

Fig. 3 illustrates the relationship between variables at each interval. Parameters and initial conditions ($b(0-,x)$, $q(0-,x)$, $w(0-)$, the minus sign represents left limits) determine outputs in each t ($B(t)$, $\sigma(t)$, $Q(t)$, $w(t)$ and $v(t)$). Provided they satisfy the transition conditions, the state changes and $b\left(T_{\{1,2\}},x\right)$, $q\left(T_{\{1,2\}},x\right)$ and $w(T_2)(=0)$ are conveyed to be the initial conditions of the next interval.

The parameters in the model are $s(t)$, $\lambda(t)$, $g(x)$, $f(x)$ and $v(t)$. Focusing on time-varying parameters, a capacity $s(t)$ and potential waiting time $v(t)$, the model can examine how $v(t)$ changes with given $s(t)$, whereas it can investigate how $s(t)$ fluctuates with fixed $v(t)$.

The actual airspace can be precisely simulated by considering two approaches in proper procedures. Firstly, key is assessing the state of the airspace with $s(t)$ fixed. This is because estimating $s(t)$ is more valid than $v(t)$ as a first step to analyze the flow based on the flight data. $s(t)$ can be deduced from the data, which elicits the arrival and exit times. Secondly, based on the result of $v(t)$ in the first step, we can check how the airspace behaves with $v(t)$ fixed at v^*. The system constantly experiences congestion, but its waiting time peaks at v^*. Furthermore, it is contemplated that the traffic flow can be analyzed more closely by changing $s(t)$ again from the outcome of the second step. Although a repeated calculation is desirable for careful analysis, this paper focuses only on the first step: given $s(t)$.

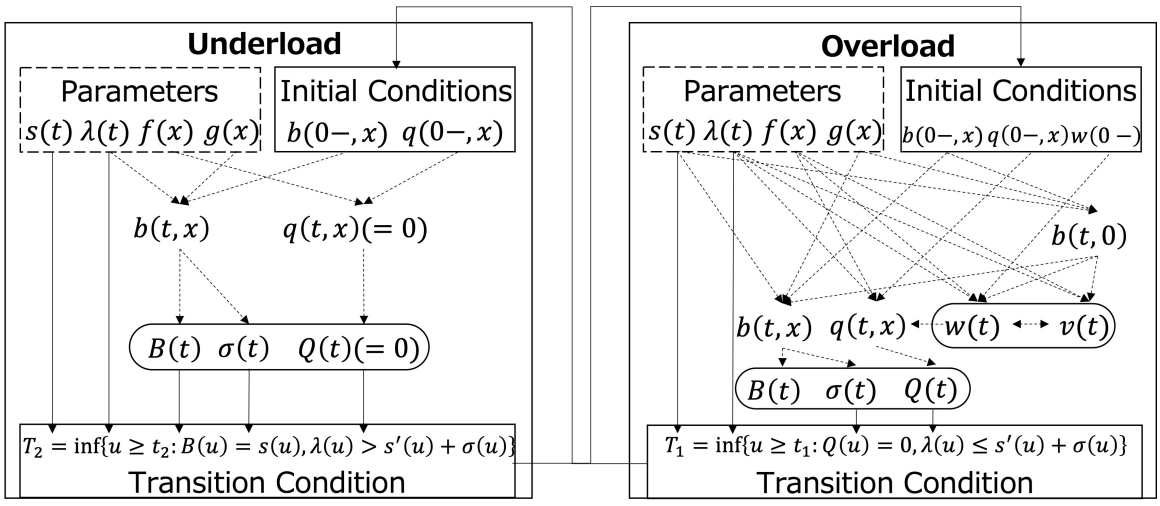

Figure 3 – Relationship between the variables at each interval with given $s(t)$.

3. Analysis of Current Arrival Flow

3.1 Targeted Airspace and Flight Data

Itoh and Mitici [13] reported that over 70% of all arrivals at Tokyo International Airport are from the southwest (red lines in Fig. 4). Itoh et al. [2] also indicated that it may be effective to control aircraft intervals and flight time in the southwest enroute airspace to prevent delays in terminal airspace. Based on these findings, the research team has conducted a preparatory analysis and hypothesized that controlling arrival intervals in the upstream airspace, 170-100 NM from a bench-mark waypoint called XAC (the green region in Fig. 4), can help relieve arrival flow congestion in the enroute airspace, 100-30 NM from the waypoint (the blue region in Fig. 4). This paper covers the latter airspace for the subsequent work, which will focus on managing the flow in the terminal airspace next to the area.

We obtain data that contain the time of passage at 100 and 30 NM from XAC for 36 days comprising 5000 aircraft (unit time: second). These figures are provided by Trajectorized En-route Traffic Data Processing System (TEPS) [14] and usable in this study. This paper restricts targets to aircraft entering the airspace after 17:00 and exiting it before 22:00 since Itoh and Mitici [5][13] indicate this period is the most congested one.

3.2 Determining Parameters for the Model

This section mentions the evidence-based setup of $\lambda(t)$, $g(x)$, $f(x)$ and $s(t)$ to analyze the current airspace. The arrival rate $\lambda(t)$ is defined as the reciprocal of the inter-arrival time between preceding and subsequent aircraft and the inter-arrival time is defined as the difference between their time of passage at 100 NM from XAC. Note that $\lambda(t)$ must be right-continuous functions with left limits to apply to the $G_t/GI/s_t + GI$ fluid model. In this paper, $\lambda(t)$ is aggregated in 10-minutes increments. For an extreme instance, $\lambda(t)$ for the virtual data in Table 1 is

$$\lambda(t) = \begin{cases} \int_0^{300} \frac{1}{300} dt + \int_{300}^{600} \frac{1}{1200} dt = 1.25 & (0 \leq t < 1) \\ \int_{600}^{1200} \frac{1}{1200} dt = 0.5 & (1 \leq t < 2) \end{cases}$$

where $t = 0$ corresponds to 17:00, $t = 1$ corresponds to 17:10, $t = 2$ corresponds to 17:20 and so on.

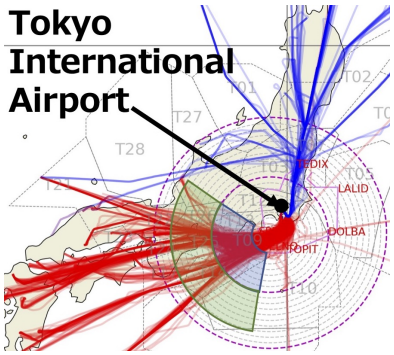

Figure 4 – Enroute airspace (the blue region) and upstream airspace (the green region).

Table 1 – Virtual flight data as an example.

Aircraft	Arrival	Exit
A	17:00:00	17:25:00
B	17:05:00	17:30:00
C	17:25:00	17:30:00

Fig. 5 is the boxplot of $\lambda_i(t)$ $(1 \leq i \leq 36)$ each day and Table 2 is the average value of representative values of $\lambda_i(t)$. For instance, the mean value of the first quantiles for 36 days is 22.3/h. In what follows, subscript i is used on parameters and outputs with each day. Some days experience very crowded arrivals, while the region have no arrivals on others, concluding that $\lambda(t)$ varies according to the day and that time-dependent arrivals in the same day can be observed. Fig. 6 is the smoothed arrival history $\lambda_{av,i}(t)$, calculated by

$$\lambda_{av,i}(t) = \frac{1}{36}\sum_{i=1}^{36}\lambda_i(t)$$

If $\lambda_i(t) = 1.6$ for 20 days and $\lambda_i(t) = 2.5$ for 16 days during the first 10 minutes, for instance,

$$\lambda_{av,i}(t) = \frac{1}{36}\left[\sum_{i=1}^{20} 1.6 + \sum_{i=21}^{36} 2.5\right] = 1.0(0 \leq t < 1)$$

In what follows, subscript av,i is used on the parameter and output with the mean on all days.

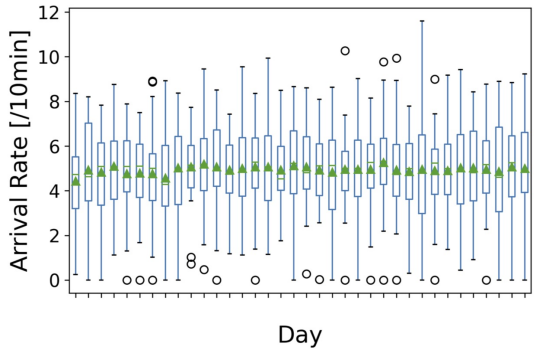

Figure 5 – Boxplot of $\lambda_i(t)$ $(1 \leq i \leq 36)$.

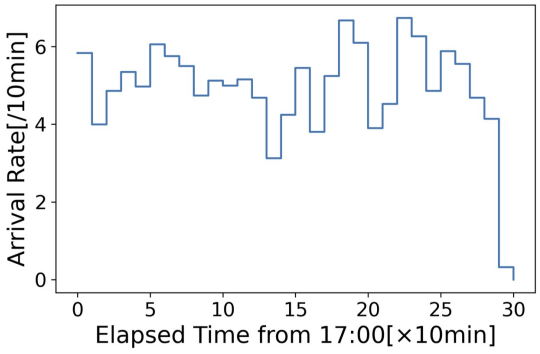

Figure 6 – History of $\lambda_{av,i}(t)$.

Table 2 – Mean value of representative values of $\lambda_i(t)$ $(1 \leq i \leq 36)$.

Averaged	[/10min]	[/h]
Mean	5.0	29.7
Standard deviation	2.0	11.9
Minimum	0.3	1.9
First quartile	3.7	22.3
Second quartile	5.0	29.8
Third quartile	6.3	37.6
Maximum	8.8	52.8

Service time is not strictly the same as flight time, the difference between the time of passage at 100 and 30 NM from XAC respectively. In this regard, however, the analysis in this paper presumes that service time is equal to flight time. The flight time distribution on all days is illustrated in Fig. 7. We consider the service time distribution $g_{av,i}(x)$ to be identical to the normal distribution $N(496.6, 46.8^2)$ when referencing Itoh et al. [2], although this assumption can be reviewed for precise analysis in future work. Based on $g_{av,i}(x)$, the abandon time distribution $f_{av,i}(x)$ is assumed to be $N(496.6 \times 1.4, 46.8^2)$. The left-hand tail of $f_{av,i}(x)$ slightly overlaps the right-hand tail of $g_{av,i}(x)$, which can reflect the scarcity of emergency circumstances like runway closing. Finally, an airspace capacity $s(t)$ is determined by $c(t)$, the number of aircraft in the airspace at time t. In this paper, $c(t)$ is aggregated in increments of 10 seconds. For the virtual flight data in Table 1, $c(t)$ is

$$c(t) = \begin{cases} 1 & (0 \leq t < 30) \\ 2 & (30 \leq t < 150) \\ 3 & (t = 150) \\ 2 & (150 \leq t < 180) \end{cases}$$

Note that unit time of $c(t)$ above is 10 seconds. Fig. 8 is the boxplot of $c_i(t)$. Here, $c_i(t)$ varies by the day and hour, while Fig. 9 is the history of $c_{av,i}(t)$ at each time t, the average number of aircraft at each specific time in the airspace:

$$c_{av,i}(t) = \frac{1}{36} \sum_{i=1}^{36} c_i(t)$$

If $c_i(t) = 3.2$ for 20 days and $c_i(t) = 5.0$ for 16 days during the first 10 seconds, for instance,

$$c_{av,i}(t) = \frac{1}{36} \left[\sum_{i=1}^{20} 3.2 + \sum_{i=21}^{36} 5.0 \right] = 4.0 (0 \leq t < 1)$$

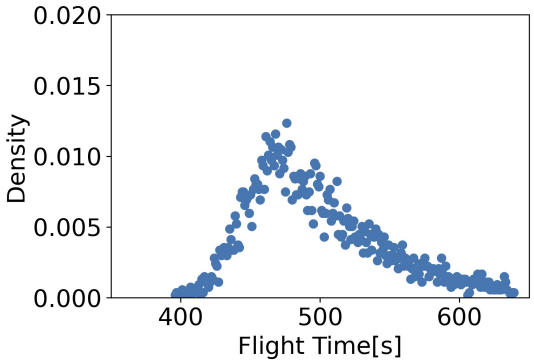

Figure 7 – Service time distribution $g_{av,i}(x)$.

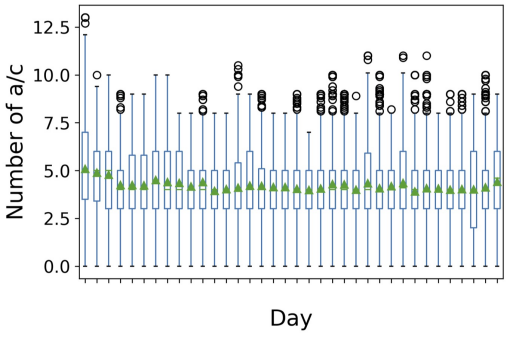

Figure 8 – Boxplot of $c_i(t)$.

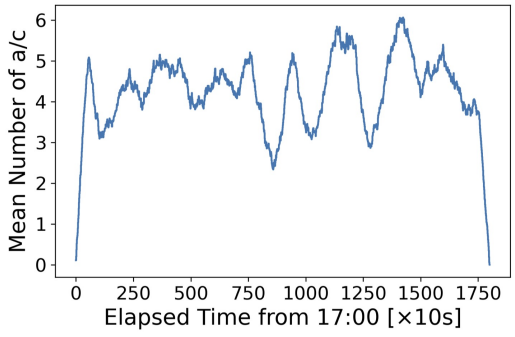

Figure 9 – History of $c_{av,i}(t)$.

3.3 Methodology for Simulating the Airspace

The functions in the $Gt/GI/st+GI$ fluid model and the actual number of aircraft in the airspace should have the following relation (cf. Fig. 2)

$$c(t) = B(t) + Q(t) + \lambda(t) - \sigma(t) - \int_0^\infty q(t,x)\frac{f(x)}{\bar{F}(x)}dx$$

where

$$\bar{F}(x) = 1 - F(x)$$

and the fifth term on the right-hand side is theoretically equal to the number of abandoned aircraft. In practical terms, that term is sufficiently smaller than $c(t)$, $B(t)$ and $Q(t)$ because of the scarcity of abandonment and $\lambda(t)$ and $\sigma(t)$ are an order of magnitude smaller than $B(t)$, $Q(t)$ and $c(t)$. Accordingly, we can conclude that the $Gt/GI/st+GI$ fluid model can simulate real airspace appropriately provided the following equation is satisfied:

$$c(t) \approx X(t) = B(t) + Q(t) \tag{1}$$

Fig. 10 is the flowchart on the procedure used to analyze the current airspace with fixed $s(t)$. Firstly, the view of airspace in the real world can be obtained by counting the number of aircraft in the airspace $c(t)$ using recorded flight data with the arrival and exit time of each aircraft. Although we cannot gain a deep insight into the arrival flow, we can roughly predict when the delay is to arise. Conversely, parameters in the $Gt/GI/st+GI$ queueing model, such as $\lambda(t)$, $g(x)$, $f(x)$ and $s(t)$, can be set up by the data, whereupon outputs in the model, like $Q(t)$ and $B(t)$, are calculated. Finally, the model can be validated by Eq.(1). This calculation should be repeated until Eq.(1) is satisfied while tuning parameters. Combining data analysis with queueing theory can elicit more insights into the time-varying characteristics of the airspace. If we rethink how best to determine parameters, we need only modify the part of the "Parameters in Queueing Model". This methodology can be employed for various types of arrival flow at general airports under proper setting of airspace.

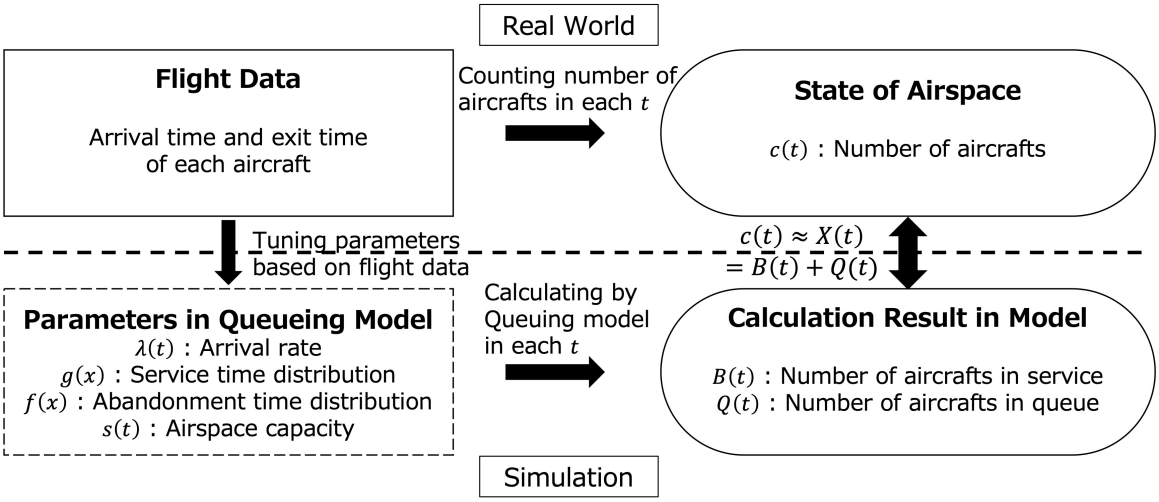

Figure 10 – Flowchart to analyze airspace.

4. Delay Time in the Current Airspace

To understand how the arrival aircraft flows, the present airspace is analyzed to calculate delay time $v_{av,i}(t)$, focusing on capacity $s_{av,i}(t)$ among the queueing model parameters. The step size in the calculation is 10 seconds, although the arrival rate $\lambda_{av,i}(t)$ is aggregated in ten-minute increments, as shown in Section 3.2. Fig. 11(a) shows the histories of $\lambda_{av,i}(t)[/10\text{s}]$, $Q_{av,i}(t)$, $B_{av,i}(t)$ and $\sigma_{av,i}(t)[/10\text{s}]$, whereas Fig. 11(b) is on $w_{av,i}(t)[\times 10\text{s}]$, $v_{av,i}(t)[\times 10\text{s}]$ and $X_{av,i}(t) = B_{av,i}(t) + Q_{av,i}(t)$, under $s_{av,i}(t) = 5.0$, $g_{av,i}(x)$ and $f_{av,i}(x)$. $c_{av,i}(t)$ is also shown with them. Note that the initial time 0 corresponds to 17:00 in the real world. The mean value, standard deviation and maximum value are listed in Table 3. Obviously, Eq.(1) is not strictly satisfied for all periods (pronounced at around 19:00 ($t = 720 \times 10\text{s}$)), but as an approximation, we can infer that the current arrival manager operates the airspace with a constant workload. Since this policy is maintained, even when the flow increases, there are two delay phases between 20:00 ($t = 1080 \times 10\text{s}$) and 21:00 ($t = 1440 \times 10\text{s}$). This is reasonable because $c_{av,i}(t)$ exceeds $5.0 = s_{av,i}(t)$ during the period. Conversely, the smooth arrival flow can be realized in the current airspace in other periods, which leads to $E[v_{av,i}(t)] = 4.6\text{s}$ despite $\max\{v_{av,i}(t)\} = 61.3\text{s}$.

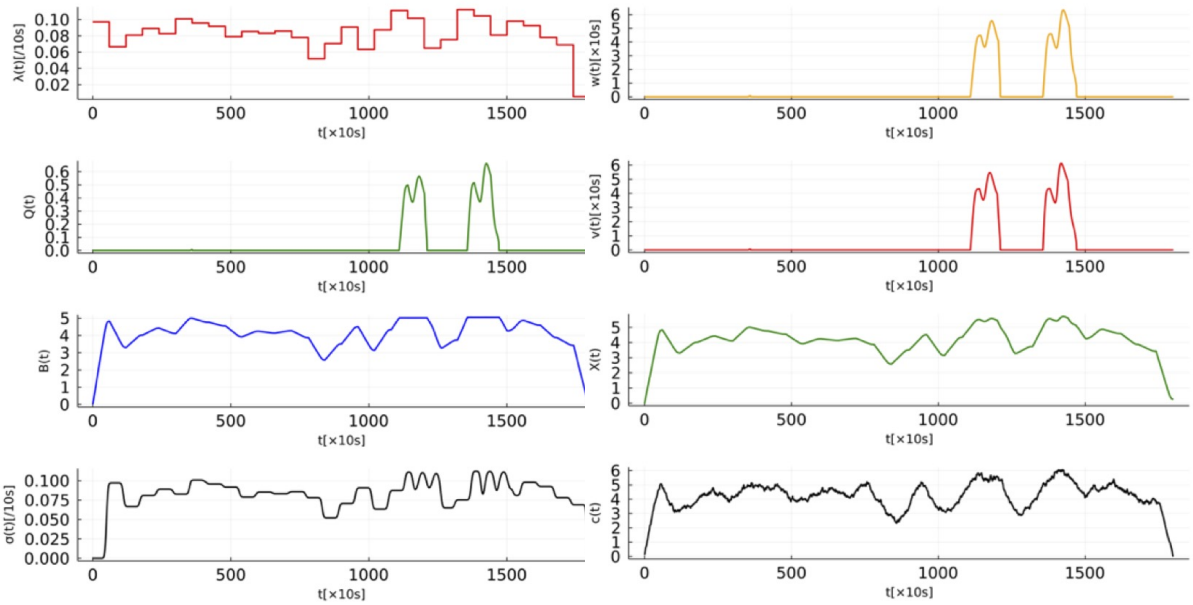

(a) $\lambda_{av,i}(t)[/10\text{s}]$, $Q_{av,i}(t)$, $B_{av,i}(t)$ and $\sigma_{av,i}(t)[/10\text{s}]$ from top to bottom

(b) $w_{av,i}(t)[\times 10\text{s}]$, $v_{av,i}(t)[\times 10\text{s}]$ and $X_{av,i}(t) = B_{av,i}(t) + Q_{av,i}(t)$ from top to bottom

Figure 11 – Calculation results in $s_{av,i}(t) = 5.0$ with $c_{av,i}(t)$, $g_{av,i}(x)$ and $f_{av,i}(x)$.

Table 3 – Representative values of functions in the actual airspace.

$s_{av,i}(t) = 5.0$	$E[\cdot]$	$\sqrt{V[\cdot]}$	$\max\{\cdot\}$
$Q_{av,i}(t)$	0.1	0.1	0.7
$B_{av,i}(t)$	4.1	0.8	5.1
$\sigma_{av,i}(t)[/\text{s}]$	0.008	0.002	0.011
$w_{av,i}(t)[\text{s}]$	4.8	13.9	63.4
$v_{av,i}(t)[\text{s}]$	4.6	13.4	61.3
$X_{av,i}(t)$	4.1	0.9	5.7

5. Discussion

As mentioned in Section 3.1, it is speculated that a more orderly arrival flow with less variance in inter-arrival time would be achievable within the enroute airspace (the blue region in Fig. 4) by controlling aircraft intervals in the upstream airspace (the green region in Fig. 4). This inference becomes more plausible given the dependency among variables in the $Gt/GI/st+GI$ fluid model (see Fig. 3). $B(t)$, $\sigma(t)$ and the transition conditions in the underloaded interval and $Q(t)$, $w(t)$, $v(t)$ and overloaded interval respectively, depend on the arrival rate $\lambda(t)$. These discussions can be summarized as follows; improving the standard deviation of $\lambda(t)$ can directly relieve delay.

Eight scenarios of virtual arrival rate $\lambda(t)$ (see Table 4) are studied to confirm scope to alleviate crowding by a sophisticated arrival flow with less variance in inter-arrival time. Firstly, two types of $\lambda(t)$ are constructed using an exponential distribution as the probability distribution function of inter-arrival time. It represents a more random and unimproved arrival flow than $\lambda_{av,i}(t)$, average traffic in the current airspace. Scenario 1 is obtained from the distribution, with a mean value of 121.2s corresponding to 29.7/h. It is the same rate as that in $\lambda_{av,i}(t)$ (see Table 2). Scenario 2 is from the distribution, whose mean value of 138.5s corresponding to 26.0/h. It is the intermediate one between 29.7/h and 22.3/h, the mean first quantile of $\lambda_i(t)$ (see Table 2). It is much less congested compared with $\lambda_{av,i}(t)$.

Secondly, six types of $\lambda(t)$ are constructed using normal distribution. This is supposed to be the ideal inter-arrival time distribution and achievable via the existing air traffic control system. In the terminal area, where aircraft intervals are highly ordered, inter-arrival time distribution can be approximated by normal distribution. As shown in Figs. 12 and 13, the distribution at 40 NM from Tokyo International Airport has a standard deviation of 41.4s, while that at 30 NM from Tokyo International Airport has a standard deviation of 25.0s. The aircraft time interval here does not follow normal distribution precisely, so we introduce distribution as an idealized scenario. Scenarios 3, 4 and 5 are obtained from normal distribution with a standard deviation of 41.4s, while Scenarios 6, 7 and 8 are gained from normal distribution with a standard deviation of 25.0s. The mean values of the arrival rate in Scenarios 4, 5, 7 and 8 are based on Scenarios 1 and 2, while those in Scenarios 3 and 6 are 31.0/h (> 28.7/h). This simulates a more crowded enroute airspace.

Table 4 – Eight scenarios of inter-arrival time distribution for $\lambda(t)$.

Mean	Exponential	Normal	
		$\sigma = 41.4$s	$\sigma = 25.0$s
$\mu = 116.1$s (31.0/h)		3	6
$\mu = 121.2$s (29.7/h)	1	4	7
$\mu = 138.5$s (26.0/h)	2	5	8

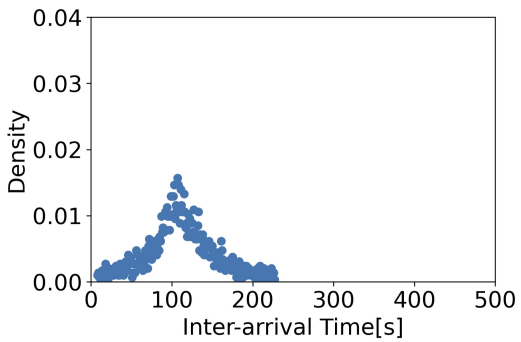

Figure 12 – Inter-arrival time distribution at 40 NM from Tokyo International Airport.

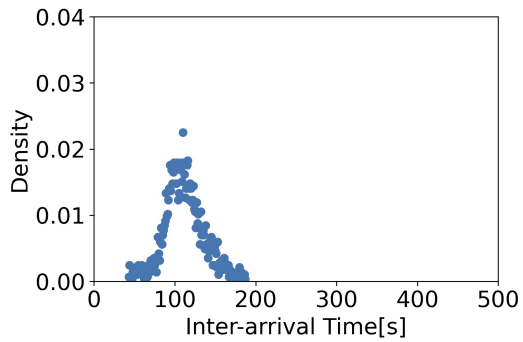

Figure 13 – Inter-arrival time distribution at 30 NM from Tokyo International Airport.

For each Scenario j ($1 \leq j \leq 8$), 100 trials are conducted. In each trial k ($1 \leq k \leq 100$), random variables are sampled to determine $\lambda_{j,k}(t)$. The mean of $v_{j,k}(t)$ ($= v_{j,k,mean}$) and the maximum of it ($= v_{j,k,max}$) are calculated using $\lambda_{j,k}(t)$;

$$v_{j,k,mean} = E\left[v_{j,k}(t)\right], v_{j,k,max} = \max\{v_{j,k}(t)\}$$

The mean and maximum values are then averaged to argue the average delay and its peak by

$$v_{j,\{mean,max\}} = \frac{1}{100}\sum_{k=1}^{100} v_{j,k,\{mean,max\}}$$

Figs. 14(a) and 14(b) illustrate the result on $v_{j,mean}$ and $v_{j,max}$, under $s_{av,i}(t)$, $g_{av,i}(x)$ and $f_{av,i}(x)$. The black line corresponds to $v_{av,i,mean}$ and $v_{av,i,max}$ in $\lambda_{av,i}(t)$ (see Table 3). The bars show a 95% confidence interval for each scenario assuming $v_{j,k,mean}$ and $v_{j,k,max}$ following normal distribution. Note that the mean arrival rate in the current airspace equates to that in Scenarios 1, 4 and 7 (29.7/h). We can deduce that the mean and maximum delay time values are basically larger in a more random and unimproved flow, even if the mean arrival rate per hour is smaller with a more random exponentially distributed inter-arrival time (Scenario 2). Moreover, comparing the line with Scenarios 4 or 7, $v_{\{4,7\},mean}$ and $v_{\{4,7\},max}$ are significantly smaller than that in current airspace, $v_{av,i,mean}$ and $v_{av,i,max}$. It derives a new finding; the airspace can become more stabilized with a more controlled arrival flow and less variance in inter-arrival time. Furthermore, even if the mean number of incoming aircraft per hour is larger than before (Scenarios 3 and 6, 31.0/h), the system can limit any accumulation of delay. In other words, a higher level of arrival management is required to accommodate additional aircraft in future. This effect is more prominent when $\sigma = 25.0$s than $\sigma = 41.4$s. Therefore, we can deduce that the arrival manager can stabilize traffic flow in the enroute airspace by controlling the upstream airspace flow in such a way as to ensure that inter-arrival time follows the distribution with less variance, particularly the ideal normal distribution.

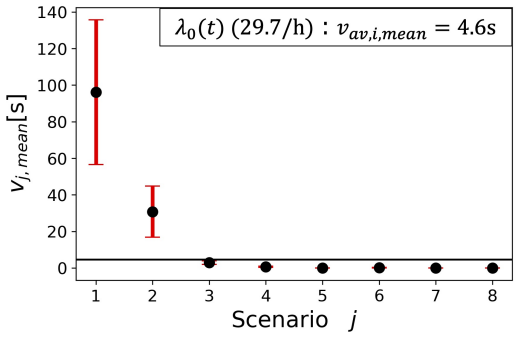

(a) $v_{j,mean}$ for each scenario, $s_{av,i}(t) = 5.0$

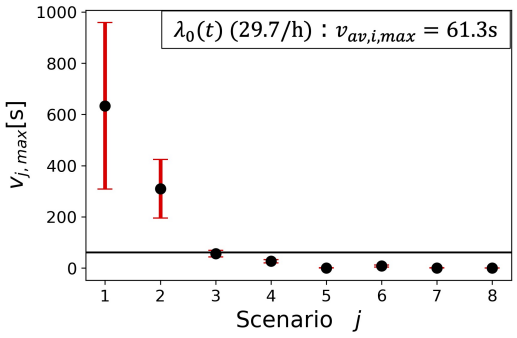

(b) $v_{j,max}$ for each scenario, $s_{av,i}(t) = 5.0$

Scenario	$v_{j,mean}$[s]	95%CI [s]
1	96.2	[56.6,135.7]
2	30.8	[16.8,44.8]
3	2.9	[1.9,3.8]
4	0.7	[0.4,1.0]
5	0.0	-
6	0.2	[0.1,0.3]
7	0.0	-
8	0.0	[0.0,0.0]

(c) $v_{j,mean}$ with confidence interval

Scenario	$v_{j,max}$[s]	95%CI [s]
1	633.6	[308.7,958.4]
2	309.5	[195.0,423.9]
3	56.6	[43.8,69.4]
4	26.6	[19.7,33.4]
5	0.6	-
6	7.9	[4.1,11.7]
7	0.7	-
8	0.0	[0.0,0.0]

(d) $v_{j,max}$ with confidence interval

Figure 14 – Results for eight scenarios.

6. Conclusion and Future Work

This paper applies a deterministic fluid model, which approximates the $Gt/GI/st+GI$ time-varying queueing model, to examine how the delay time in the enroute airspace is reduced by an earlier control of its upstream airspace. This is positioned as part of preliminary preparation of the study that aims to propose strategies for air traffic control to mitigate congestion by aircraft arriving at Tokyo International Airport in the terminal airspace.

As a methodology for analyzing arrival flow by the model in detail, we suggest matching the number of aircraft in the airspace from actual flight data against calculation results from the model using parameters estimated by the data. As a result of analyzing the actual airspace, there is no delay in almost all periods except those between 20:00 and 21:00 in the current enroute airspace.

Moreover, given speculation on the relationship between variables on the model, an experiment is conducted to ascertain whether controlling the arrival rate, or spacing adjustment in the more upstream region (the green region in Fig. 4), can stabilize the enroute airspace. The result indicates that E-AMAN should intervene in the traffic flow of the upstream airspace for the inter-arrival time of the aircraft to follow the distribution with less variance such as the normal distribution.

Future work will focus on analyzing the current terminal area within 80 NM of Tokyo International Airport. Subsequently, based on the knowledge obtained by this paper, we will verify the hypothesis that a more orderly exit flow from the terminal airspace could be attained by controlling the arrival flow at enroute airspace $\lambda(t)$. It is derived from the following consideration (see Fig. 15); from the additional analysis in Section 5, more sophisticated $\lambda(t)$ reduces $v(t)$. Moreover, it can stabilize $\sigma(t)$, which is the 'exit rate' from the enroute airspace (see Scenarios 4 or 7 in Figs. 16 and 17 and compare with the black line). Since this orderly $\sigma(t)$ can be identical to $\lambda_T(t)$, the arrival rate at the terminal airspace, congestion is also mitigated in the area.

If this tentative theory is correct, a smoother landing flow could be achieved to ease overcrowding at surface and departure and we would be able to establish framework of a structured approach from E-AMAN's / Multi-Stage AMAN's perspective in the integrated operation around airports.

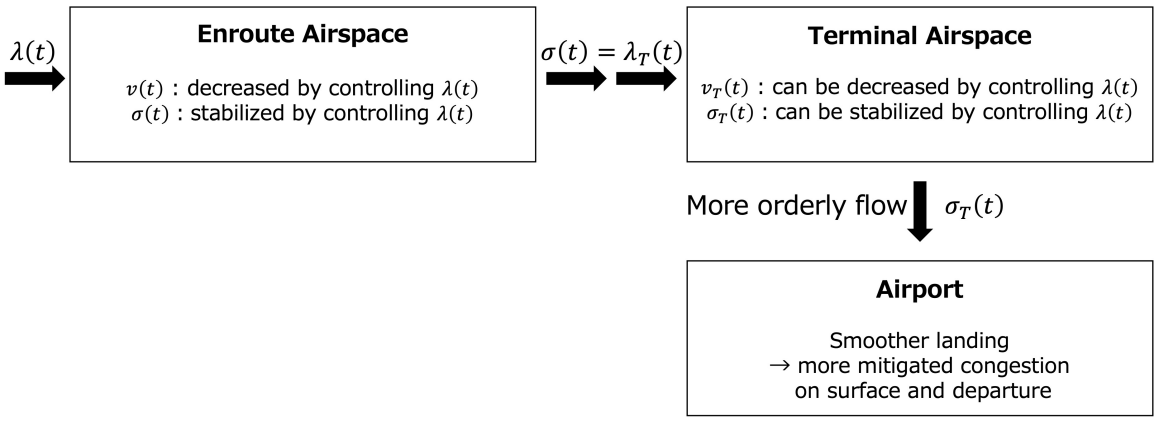

Figure 15 – Arrival and departure flows in airport and surrounding airspaces.

7. Acknowledgement

This research was supported by a Grant-in-Aid for Scientific Research (20H04237). We would like to express our sincere appreciation for the data and technical support provided by the Civil Aviation Bureau of the Ministry of Land, Infrastructure, Transport and Tourism.

8. Contact Author Email

mail to: {higasa-koki, eriitoh}@g.ecc.u-tokyo.ac.jp

9. Copyright Statement

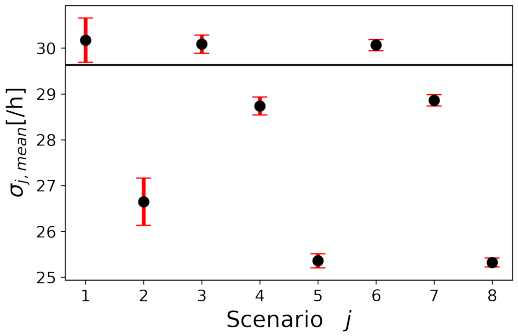

Figure 16 – $\sigma_{j,mean}$ for each scenario, $s_{av,i}(t) = 5.0$.

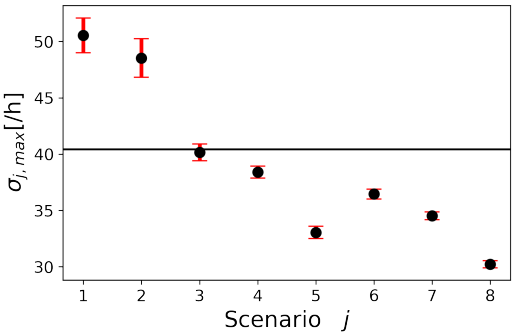

Figure 17 – $\sigma_{j,max}$ for each scenario, $s_{av,i}(t) = 5.0$.

References

[1] Japan Aircraft Development Corporation. Worldwide Market Forecast 2020-2040. Retrieved May 1, 2022, from http://www.jadc.jp/files/topics/166_ext_01_en_0.pdf, 2021

[2] Itoh E., Miyazawa Y., Finke M. and Rataj J. Macroscopic Analysis to Identify Stage Boundaries in Multi-Stage Arrival Management. *ENRI International Workshop on ATM/CNS(pp. 59-76)*. Springer, Singapore, 2019.

[3] Itoh E., Brown M., Senoguchi A., Wickramasinghe N. and Fukushima S. Future arrival management collaborating with trajectory-based operations. *Air Traffic Management and Systems II(pp. 137-156)*. Springer, Tokyo, 2017.

[4] Shone R, Glazebrook K and Zografos K. Applications of stochastic modeling in air traffic management: Methods, challenges and opportunities for solving air traffic problems under uncertainty. *European Journal of Operational Research*, Vol. 292, No. 1, pp 1-26, 2021.

[5] Itoh E and Mitici M. Analyzing tactical control strategies for aircraft arrivals at an airport using a queuing model. *Journal of Air Transport Management*, Vol. 89, No. 101938, 2020.

[6] Pyrgiotis N, Malone K and Odoni A. Modelling delay propagation within an airport network. *Transportation Research Part C: Emerging Technologies*, Vol. 27, pp. 60-75, 2013.

[7] Jacquillat A and Odoni A. An integrated scheduling and operations approach to airport congestion mitigation. *Operations Research*, Vol. 63, No. 6, pp. 1390-1410, 2015.

[8] Shone R, Glazebrook K and Zografos K. Resource allocation in congested queueing systems with time-varying demand: An application to airport operations. *European Journal of Operational Research*, Vol. 276, No. 2, pp. 566-581, 2019.

[9] Caccavale M, Iovanella A, Lancia C, Lulli G and Scoppola B. A model of inbound air traffic: The application to Heathrow airport. *Journal of Air Transport Management*, Vol. 34, pp. 116-122, 2014.

[10] Gwiggner C and Nagaoka S. Data and queueing analysis of a Japanese air-traffic flow. *European Journal of Operational Research*, Vol. 235, No. 1, pp. 265-275, 2014.

[11] Itoh E, Mitici M and Schultz M. Modeling Aircraft Departure at a Runway Using a Time-Varying Fluid Queue. *Aerospace*, Vol. 9, Issue. 3, No.119, 2022.

[12] Liu Y and Whitt W. The G t/GI/st+ GI many-server fluid queue. *Queueing Systems*, Vol. 71, No. 4, pp. 405-444, 2012.

[13] Itoh E and Mitici M. Evaluating the impact of new aircraft separation minima on available airspace capacity and arrival time delay. *The Aeronautical Journal*, Vol. 124, No. 1274, pp. 447-471, 2020.

[14] Ministry of Land, Infrastructure, Transport and Tourism. On the revision of control service processing rule concerning Trajectorized En-route Traffic Data Processing System (TEPS) (in Japanese). Retrieved May 1, 2022, from https://www.japa.or.jp/wp-content/uploads/2018/11/cab20181001-3.pdf, 2018